LU-TP 21-17
June 9, 2021

# Resolving Quasi-Degenerate Higgs Bosons

**Gustav Lindberg**

Department of Astronomy and Theoretical Physics, Lund University

Bachelor thesis supervised by Johan Rathsman and Jonas Wittbrodt


LUND
UNIVERSITY

# Popular Science Description

Currently, scientists have managed to explain most things that happen in nature with only a limited number of fundamental particles. However, some things remain unexplained, such as dark matter. Dark matter is matter that has not been observed but is still known to exist and have mass because of the gravitational force it exerts on stars and galaxies. Dark matter is one of the greatest mysteries in physics since we know almost nothing about it. This, together with other unexplained phenomena, seems to be an indication that there are more particles than those discovered so far.

The latest fundamental particle that has been discovered is the so-called Higgs boson, which explains why other particles have mass. Imagine that particles are like balloons. If you leave them alone, they will fly away because they are so light. Now imagine Higgs bosons are like stones that you attach to some of these balloons. The balloons that you attached stones to will become heavier and not fly away. This corresponds to particles such as protons and electrons having mass. However, balloons that do not have any stones attached to them still fly away. An example of this is light, which does not interact with the Higgs boson and therefore has no mass.

So far, we have only found one type of Higgs boson. However, scientists believe that finding new types of Higgs bosons could be a step towards explaining dark matter. The new Higgs bosons cannot actually be dark matter because they would quickly decay into known particles, but they can give mass to dark matter, in the same way as the known Higgs boson gives mass to everyday matter.

However, so far, experiments have only detected one Higgs boson. If other Higgs bosons exist, there must be a reason why experiments have not detected them. One reason could be that the new Higgs bosons have masses very similar to the one already detected, meaning that even though they in fact are different, they might still look identical to the experiments. The goal of this thesis is to determine exactly how similar these new Higgs bosons can be to the one already found, while still not being detected as a separate particle. Setting limits on the properties of the new Higgs bosons can be important for scientists who want to search for them, and searching for these new Higgs bosons could be a way to indirectly search for a way to explain dark matter.

Therefore, this thesis can be useful to the search for additional Higgs bosons, which might be useful for solving one of the greatest mysteries in physics, namely dark matter.

**Abstract**

Many models beyond the Standard Model that predict the existence of multiple Higgs bosons. In general, some of these additional Higgs bosons could be quasi-degenerate in mass either to each other or to the observed 125 GeV Higgs boson. The goal of this thesis is to study under which circumstances we can resolve such Higgs bosons. We first make the simplifying assumption that the observed and predicted invariant mass distributions are exact Gaussians, and use a $\chi^2$ test to determine how closely a combination of several particles resembles a single particle. We find that quasi-degenerate Higgs bosons with similar couplings are unlikely to be resolved by the experiments if their mass separation is less than twice the experimental resolution. We validate our findings by running Monte Carlo simulations of several important Higgs processes, and we find that the Gaussian approximation provides a decent description of when quasi-degenerate particles are resolvable. We finally consider interference effects in order to study cases where Higgs bosons have a much larger decay width than the Standard Model Higgs boson. We find that interference can make it significantly easier or significantly harder to resolve the two Higgs bosons, depending on the parameters of the model.

# Contents

# 1 Introduction

In 2012, the ATLAS and CMS collaborations at the LHC discovered a new boson with a mass of 125 GeV [1, 2] which was later confirmed to be the Higgs boson. Since then, the LHC has been conducting many new searches and measurements in order to learn more about the Higgs sector.

While the Standard Model works with just one Higgs boson, and the experiments have not found any strong hints for additional Higgs bosons, there are several well-motivated models beyond the Standard Model that require multiple Higgs bosons. This is especially true for several models attempting to solve dark matter [3] and supersymmetry [4], which require introducing multiple Higgs bosons.

No Higgs bosons other than the Standard Model one have been found though. One explanation for this could be that they are so close in mass to the Standard Model Higgs boson that it is very difficult to tell the difference between the new Higgs bosons and the Standard Model one, which is what is meant by quasi-degenerate. Another explanation could be that the new Higgs bosons could be at masses that have not yet been studied in experiments or have rates beyond the reach of current analyses. However, also in this case it is also possible to have multiple Higgs bosons which are too close to each other to be resolved individually, but clearly distinct from the Standard Model Higgs boson.

The conceptually simplest LHC Higgs searches and measurements, in particular in the $H \to \gamma\gamma$ [5, 6] and $H \to ZZ \to 4l$ [7, 8] final states, consist of searching for bumps in invariant mass spectra. When a single particle is detected, after subtracting all backgrounds, the invariant mass plot typically looks like a Gaussian centered at the mass of the particle. The goal of this thesis is to quantify which properties of multiple Higgs bosons would result in a distribution looking like a single Gaussian.

There are two reasons why the events are distributed as a Gaussian around the mass of the particle and are not simply all located at the exact mass of the particle. The first reason, which is the main reason in the case of the Standard Model Higgs boson, is that the detectors can detect energies that are slightly off. For example, the detector may miss some particles either because they do not have enough energy to be detected or because they escape through regions the detector does not cover. Additional particles may also be falsely considered as decay products just because they hit the detector by chance. Therefore even if the particles that are detected have an energy exactly equal to the mass of the Higgs boson, the detector may detect an energy slightly smaller or slightly greater than the actual energy of the particle. Additionally, the detector itself is not perfect, so even if it were to detect all the relevant particles and no additional particles, the energy can still be off due to detector imperfections.

The other reason is that particles with a finite lifetime do not have one given mass, but can instead have a mass that is slightly larger or slightly smaller than the on-shell mass of the particle. The probability distribution of the mass of a particle with a finite lifetime $t$ is given by a Gaussian with a variance equal to

$$\Gamma = \frac{\hbar}{t}. \tag{1.1}$$

$\Gamma$ is called the total decay width of the particle.

Predictions for collider searches and measurements rely on Monte Carlo simulations of the underlying physical processes. Decays of Higgs bosons (and any other unstable particles) can be simulated in three stages: the generator level, the hadron level and the reconstruction level. Generator level simulations only include the so-called hard processes, which means that in the case of the $H \to b\bar{b}$ decay, the final state of the generator level simulations will be a $b$ quark and a $\bar{b}$ antiquark which have not yet hadronized, decayed, formed jets, or interacted in any other way.

Hadron level simulations include not only the hard processes, but also what happens to the decay products between the time they are created and the time they reach the detector. This includes

(but is not limited to) quarks and gluons hadronizing and forming jets, particles losing energy through bremsstrahlung, unstable particles decaying, etc.

Reconstruction level simulations, in addition to all the processes described above, also include detector effects. This means that reconstruction level simulations will randomly smear the energies of the particles to account for the fact that detectors may detect slightly higher or slightly lower energies for the reasons explained above. Reconstruction level simulations can also include other detector effects, for example errors in determining which type of quark or gluon produced a jet. Therefore, reconstruction level simulations show what we would actually see in a detector after removing background and noise.

When two particles are close in mass, it can also be important to take into account interference, a concept that will be explained later. In most of this thesis, we will ignore interference effects, but we will look into that at the end.

In section 2, we will use the simplifying assumption that the bumps produced by Higgs bosons are exact Gaussians in order to determine which combinations of Higgs bosons will look like a single Gaussian. We will then in section 3 run simulations to compare this to how the bumps would actually look. Finally, in section 4, we will look into what effects interference can have on this. We will conclude in section 5.

# 2 A Simplified View of Overlapping Higgs Bosons

We approximate the actual distribution observed in the experiments by the convolution of the mass distribution of the particle and a Gaussian representing experimental uncertainties. A Gaussian distribution is defined as

$$g(x) = Ae^{-\frac{(x-\mu)^2}{2s^2}} \tag{2.1}$$

where $A$ is the amplitude, $s$ is the variance and $\mu$ is the average. The convolution of two functions $S_m$ and $S_d$ is defined as

$$(S_m * S_d)(E) = \int_{-\infty}^{\infty} S_m(E')S_d(E - E')dE'. \tag{2.2}$$

In this case, $S_m$ is the mass distribution of the particle, which is a Gaussian with $\mu = m$ and $s = \Gamma$, where $m$ is the on-shell mass of the particle and $\Gamma$ is its decay width. $S_d$ is a Gaussian representing experimental uncertainties, with $\mu = 0$ and $s = r$, where $r$ is the experimental mass resolution. The convolution of two Gaussians is another Gaussian, which is why for Gaussian signal distributions signal mass distributions observed by the experiments look like Gaussians.

The signal models used in Higgs searches and measurements by the LHC collaborations are usually similar to a single Gaussian, which is appropriate for fitting a single particle (in reality more complicated functions than Gaussians are usually used, for example double-sided crystal balls or relativistic Breit-Wigner functions, see e.g. reference [6]). However, if there are multiple Higgs bosons, it would be more appropriate to fit a sum of two Gaussians rather than a single Gaussian. Depending on the parameters of the two Gaussians, a sum of two Gaussians may look like a single Gaussian. This would mean that the combined signal distribution of the two particles looks like that of a single particle to the experiment. The goal of this section is to quantify which properties of multiple Higgs bosons would result in a distribution looking like a single Gaussian.

## 2.1 Narrow-Width Approximation

The Standard-Model Higgs boson is predicted to have a decay width of $\Gamma = 4\,\text{MeV}$. Higgs searches and measurements at the LHC typically have a mass resolution $r$ around a few GeV, which means

that $\Gamma \ll r$. Therefore, for the Standard Model Higgs boson, $\Gamma \approx 0$ is a reasonable approximation. This approximation is called the narrow-width approximation.

The mass distribution $S_m$ of a particle with $\Gamma = 0$ would be a Gaussian with variance zero and infinite amplitude, which corresponds to the Dirac delta function. The delta function has the property that for any function $f$

$$\int_{-\infty}^{\infty} f(E')\delta(E')dE' = f(0). \tag{2.3}$$

Using this, we can calculate the convolution of the delta function with $S_d$:

$$\begin{aligned}(\delta * S_d)(E) &= \int_{-\infty}^{\infty} \delta(E')S_d(E - E')dE' \\ &= S_d(E).\end{aligned} \tag{2.4}$$

Therefore, a particle with mass $m$ for which the narrow-width approximation is valid will be detected by the experiments as a Gaussian shape with $\mu = m$ and $s = r$, where $r$ is the experimental resolution.

Assuming there are two Higgs bosons with masses $m_1$ and $m_2$, the distribution detected by experiments will be equal to

$$S(E) = A_1 e^{-\frac{(E-m_1)^2}{2r^2}} + A_2 e^{-\frac{(E-m_2)^2}{2r^2}}. \tag{2.5}$$

We assume without loss of generality that $m_1 \leq m_2$. In principle $r$ depends on the mass of the Higgs boson, but for the small mass differences that we are interested in we can assume that $r(E)$ is constant over the considered energy range. Therefore, we can assume that $r$ will be the same in both cases.

The amplitudes $A_1$ and $A_2$ are proportional to the number of events $N_1$ and $N_2$ involving each particle. The number of events $N_j$ involving a given particle $j$ is equal to

$$N_j = L_{\text{int}}\sigma_j \tag{2.6}$$

where $\sigma_j$ is the cross section of the signal processes involving the particle and $L_{\text{int}}$ is the integrated luminosity of the accelerator. Since $L_{\text{int}}$ is a property of the accelerator and not of the particle, this means that the amplitudes $A_1$ and $A_2$ are proportional to the cross sections $\sigma_1$ and $\sigma_2$ of each Higgs boson, with a proportionality constant which is the same in both cases. Therefore, equation (2.5) can be rewritten as

$$S(E) = L_{\text{int}}\left(\sigma_1 e^{-\frac{(E-m_1)^2}{2r^2}} + \sigma_2 e^{-\frac{(E-m_2)^2}{2r^2}}\right) \tag{2.7}$$

where $L_{\text{int}}$ and $r$ are properties of the accelerator or detector and $m_1$, $m_2$, $\sigma_1$ and $\sigma_2$ are properties of the Higgs bosons.

To incorporate the experimental assumption that there is only one particle, we fit a single Gaussian to the distribution given in equation (2.7). If the fit is good enough, then two Higgs bosons with the given properties would give rise to a distribution that looks like a single Gaussian, which would be consistent with experimental assumptions. On the other hand, if the fit is not good enough, then the two Higgs bosons would appear as two separate Gaussians, which would not be consistent with the experiments. In order to quantify which fits are good and which are not, we use a $\chi^2$-test. $\chi^2$ is defined as

$$\chi^2 = \frac{1}{n - N}\sum_E \frac{(S(E) - g(E))^2}{(\Delta S(E))^2} \tag{2.8}$$

where $n$ is the number of values for $E$ that we sum over, which corresponds to the number of bins if it were a histogram. $N$ is the number of free parameters for the Gaussian fit, $S(E)$ is the distribution given in equation (2.7), $g(E)$ is the fitted Gaussian, and $\Delta S(E)$ is the uncertainty.

We fit the two parameters $\mu$ and $s$ while fixing the number of events $N_{\text{evts}} = L_{\text{int}}(\sigma_1 + \sigma_2)$. Since the number of events $N_{\text{evts}}$ and the amplitude $A$ are related by

$$N_{\text{evts}} = \int_{-\infty}^{\infty} S(E)dE = \int_{-\infty}^{\infty} Ae^{-\frac{(E-\mu)^2}{2s^2}} dE = As\sqrt{2\pi}, \tag{2.9}$$

this means that $A$ must be equal to $\frac{L_{\text{int}}}{s\sqrt{2\pi}}(\sigma_1 + \sigma_2)$. The reason we keep the number of events constant because it is easy to tell how many events there have been without fitting anything.

This means that in our case, in equation (2.8), the number of free parameters for the Gaussian fit is $N = 2$.

We chose the uncertainty $\Delta S(E)$ in an arbitrary way so that curves that barely look like Gaussians have $\chi^2 \approx 1$, which results in an uncertainty equal to $\Delta S(E) = \frac{A_1+A_2}{75}$, or an uncertainty of 1.3% of the total amplitude. This uncertainty is probably smaller than what is realistically achievable in experiments, so we conclude that if $\chi^2 < 1$, the two Higgs bosons are unlikely to be resolved by experiments. While experimental results may still look like a single particle at $\chi^2$ slightly greater than 1 since the experimental uncertainties are probably larger, we choose to be safe in order not to apply an analysis to an edge case where we are not sure if the assumptions hold or not.

In principle, equation (2.7) has six parameters. However, we can reduce the number of free parameters since some of them do not influence the relevant properties of the fitted Gaussian.

First of all, we can drop the parameter $L_{\text{int}}$, since we do not care about the overall normalization of the event count. Also, we can include $\sigma_2$ in the overall normalization so that the coefficients in front of the exponentials are 1 and $\frac{\sigma_1}{\sigma_2}$ instead of $\sigma_1$ and $\sigma_2$. Therefore, we can replace the three parameters $L_{\text{int}}$, $\sigma_1$ and $\sigma_2$ by a single parameter $\frac{\sigma_1}{\sigma_2}$.

Similarly, we can also reduce the three parameters $m_1$, $m_2$ and $r$ into a single parameter. This is because it does not matter if we shift the distribution to the left or to the right, we can always recenter the fitted Gaussian to compensate for the shifting. Therefore, we can replace the two parameters $m_1$ and $m_2$ by a single parameter $\Delta m = m_2 - m_1$. Also, if we squeeze or stretch the sum of two Gaussians, we can always adjust the variance of the fitted Gaussian to compensate for that, so we can replace the two parameters $\Delta m$ and $r$ by a single parameter $\frac{\Delta m}{r}$. Therefore, we can reduce the three parameters $m_1$, $m_2$ and $r$ into a single parameter $\frac{\Delta m}{r}$.

So we only have two parameters which can impact the value of $\chi^2$, which are the ratio of cross sections $\frac{\sigma_1}{\sigma_2}$ and the mass difference in units of the experimental resolution $\frac{\Delta m}{r}$. We can fix all other parameters to arbitrary values since they will not impact the value of $\chi^2$. We set the weighted average mass to 125 GeV and the experimental resolution to 1.5 GeV.

We can therefore plot $\chi^2$ as a function of these two parameters, as shown in figure 2.1. Blue means that the given properties of the two Higgs bosons appear consistent with the assumption of a single particle, red means that they do not.

We can see that if $\Delta m < r$ or if $\frac{1}{20} < \frac{\sigma_1}{\sigma_2} < 20$, fitting one Gaussian to the sum of two Gaussians gives a very small value for $\chi^2$, which means that pairs of Higgs bosons having those properties are consistent with experiments assuming a single-particle signal.

The fact that small mass differences give a small $\chi^2$ is because if the mass difference is very small, then the two Gaussians will be very close together and will look like a single Gaussian, as shown in figure 2.2a.

The fact that large cross section ratios give a small $\chi^2$ is because if one of the Gaussians is much larger than the other one, the smaller Gaussian will be negligible compared to the larger Gaussian,

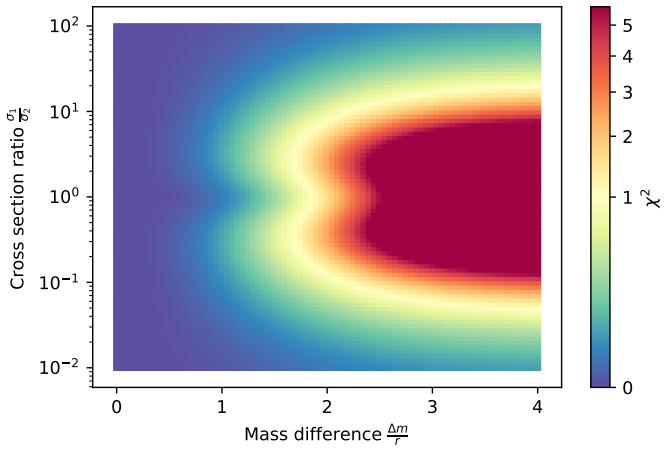


Figure 2.1: $\chi^2$ of the Gaussian fit as a function of the cross section ratio $\frac{\sigma_1}{\sigma_2}$ and the mass difference in units of the experimental resolution $\frac{\Delta m}{r}$.

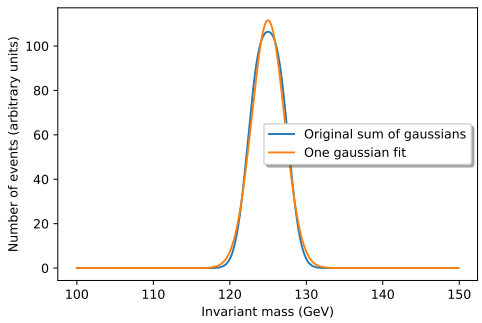


(a) $\frac{\Delta m}{r} = 1.8$, $\frac{\sigma_1}{\sigma_2} = 1$, $\chi^2 = 0.89$

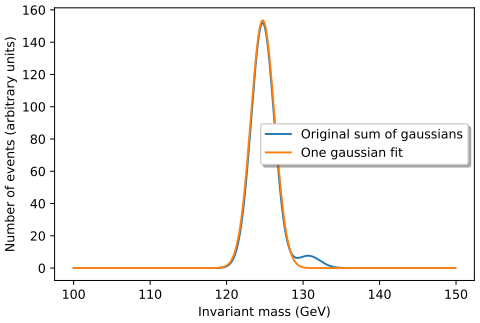


(b) $\frac{\Delta m}{r} = 4$, $\frac{\sigma_1}{\sigma_2} = 20$, $\chi^2 = 1.03$

Figure 2.2: Sums of Gaussians for different values for $\frac{\Delta m}{r}$ and $\frac{\sigma_1}{\sigma_2}$ and the corresponding Gaussian fit. We assume that the weighted average mass of the two Higgs bosons is 125 GeV and that the experimental resolution is 1.5 GeV.

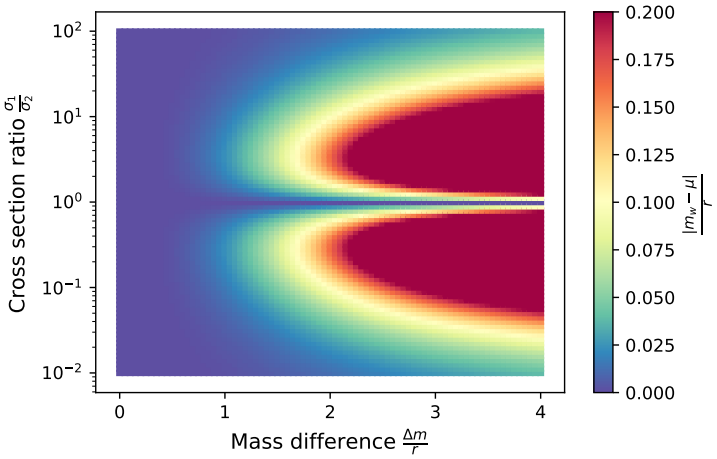


Figure 2.3: Difference between the weighted mass average $m_w$ and the center $\mu$ of the fitted Gaussian as a function of the cross section ratio $\frac{\sigma_1}{\sigma_2}$ and the mass difference in units of the experimental resolution $\frac{\Delta m}{r}$.

meaning that the sum will look very much like if there only was the larger Gaussian, as shown in figure 2.2b.

Experiments have measured that the mass of the Higgs boson is around 125 GeV. However, if there are two Higgs bosons, the center of the fitted Gaussian does not correspond to the mass of "the" Higgs boson since there are several of them. Similarly, if experiments in the future detect a bump at some other energy which in fact corresponds to multiple Higgs bosons, the center of that fitted Gaussian will not correspond to the exact mass of one Higgs boson. Therefore, it can be useful to know what the mass measured by the experiments corresponds to in the case where there are two Higgs bosons.

We define the weighted mass $m_w$ of the two Higgs bosons as

$$m_w = \frac{\sigma_1 m_1 + \sigma_2 m_2}{\sigma_1 + \sigma_2} \tag{2.10}$$

where the $\sigma_1$, $\sigma_2$, $m_1$ and $m_2$ are the cross-sections and masses of the two Higgs bosons, respectively. We can plot the difference between this weighted average and the center $\mu$ of the fitted Gaussian as a function of the two parameters $\frac{\sigma_1}{\sigma_2}$ and $\frac{\Delta m}{r}$, as shown in figure 2.3.

If we compare figures 2.1 and 2.3, we can see that all the areas that have a small value for $\chi^2$ also have a small value for $|m_w - \mu|$. Therefore, if the two Higgs bosons have properties that are consistent with the assumption of a single particle, then the approximation

$$\mu \approx \frac{\sigma_1 m_1 + \sigma_2 m_2}{\sigma_1 + \sigma_2} \tag{2.11}$$

is a fairly good approximation. This means that if there are two Higgs bosons around 125 GeV, then their rate-weighted average mass would correspond to the observed Higgs boson mass of 125.09 GeV. This approximation is actually used in fitting tools such as HiggsSignals [9] to include contributions of multiple Higgs bosons to mass measurements.

## 2.2 Non-zero Decay Width

While the narrow-width approximation is a good approximation for the Standard Model Higgs boson, some models beyond the Standard Model predict the existence of Higgs bosons with a

significantly larger decay width that is not negligible compared to the experimental mass resolution. Therefore, it can be useful to consider the case where Higgs bosons have a non-zero decay width.

Now that the mass distributions of the Higgs bosons are no longer delta functions but Gaussians with a non-zero width, the bump detected by the experiments is no longer a Gaussian convoluted with a delta function but the convolution of two Gaussians. If we solve the integral in equation (2.2) where $f$ and $g$ are both Gaussians with parameters $A_1$, $s_1$, $\mu_1$ and $A_2$, $s_2$, $\mu_2$ respectively, we find that the convolution of two Gaussians is another Gaussian with parameters equal to

$$\mu = \mu_1 + \mu_2 \tag{2.12}$$

$$s = \sqrt{s_1^2 + s_2^2} \tag{2.13}$$

$$A = A_1 A_2 s_1 s_2 \sqrt{\frac{2\pi}{s_1^2 s_2^2}} \tag{2.14}$$

In the case of the Gaussian corresponding to a Higgs boson, we must have $\mu = m_H$ where $m_H$ is the mass of the given Higgs boson ($\mu_2$ is always zero since it corresponds to the smearing due to detector effects). Also, we do not fix $A_1$ and $A_2$, but rather $\frac{A}{s}$, since that is what corresponds to the number of events. Therefore, the only parameter that changes compared to before is $s$. Since one of the Gaussians in the convolution corresponds to the experimental uncertainty and has $s_1 = r$ (as before), and the other Gaussian corresponds to the Higgs boson having a non-zero decay width and has $s_2 = \Gamma$, equation (2.13) gives us

$$s = \sqrt{r^2 + \Gamma^2} \tag{2.15}$$

where $r$ is the experimental resolution and $\Gamma$ is the decay width of the Higgs boson. If $\Gamma = 0$, this simplifies to $s = r$, which is the equation we used when we were using the narrow-width approximation.

The difference between this case and the previous section is that while the experimental resolution is the same for both Higgs bosons, both Higgs bosons do not necessarily have the same decay width. Therefore, while in the narrow-width approximation both Gaussians had the same variance $s = r$, now the Gaussians do not need to have the same variance. Therefore we now have three parameters instead of two: the cross-section ratio $\frac{\sigma_1}{\sigma_2}$, the mass difference in units of the variance of the one of the bumps $\frac{\Delta m}{\sqrt{r^2+\Gamma_1^2}}$, and the ratio of the variances of the bumps $\frac{\sqrt{r^2+\Gamma_2^2}}{\sqrt{r^2+\Gamma_1^2}}$.

We can plot $\chi^2$ as a function of these three parameters by making a 3D-plot where each axis corresponds to one parameter and color the plot to show the value of $\chi^2$ at each point, as shown in figure 2.4.

The case where the variance ratio $\frac{\sqrt{r^2+\Gamma_2^2}}{\sqrt{r^2+\Gamma_1^2}}$ is equal to 1 is equivalent to the case where we used the narrow-width approximation, since this means that both Gaussians have the same variance. This is because even if the decay width of the Higgs bosons is non-zero, if they have the same decay width, we can always define an effective experimental resolution $r' = \sqrt{r^2 + \Gamma^2}$, which gives us the same result as using the narrow-width approximation. Therefore, as expected, the pattern in the plane with $\frac{\sqrt{r^2+\Gamma_2^2}}{\sqrt{r^2+\Gamma_1^2}} = 1$ in figure 2.4 (which is at the bottom of the 3D plot and therefore not directly visible) are the same pattern as the one in figure 2.1.

We also see that if we increase the variance ratio, $\chi^2$ gets larger as long as the cross section ratio is not too large. This is because if the two Gaussians have different variances, even if they are very close together, their sum will not be a Gaussian as we can see in figure 2.5. If the cross section ratio is very large however, one of the Gaussians will always be negligible compared to the other, so $\chi^2$ will still be small.

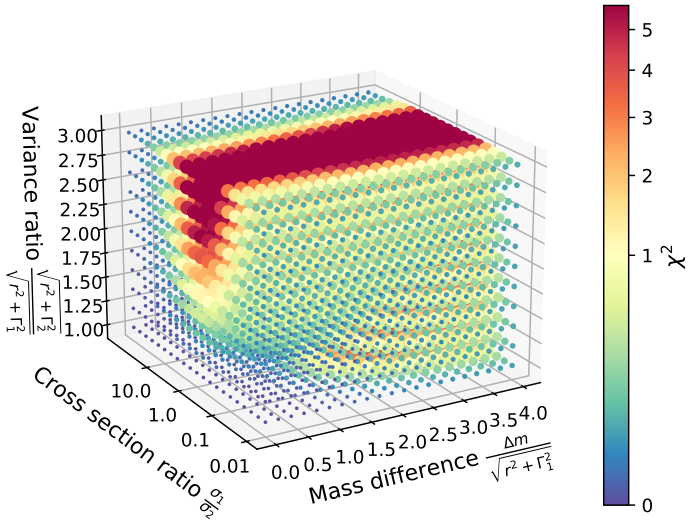


Figure 2.4: $\chi^2$ of the Gaussian fit as a function of the cross section ratio $\frac{\sigma_1}{\sigma_2}$, the mass difference in units of the variance of one of the bumps $\frac{\Delta m}{\sqrt{r^2+\Gamma^2}}$ and the ratio of the variance of the two bumps $\frac{\sqrt{r^2+\Gamma_2^2}}{\sqrt{r^2+\Gamma_1^2}}$.

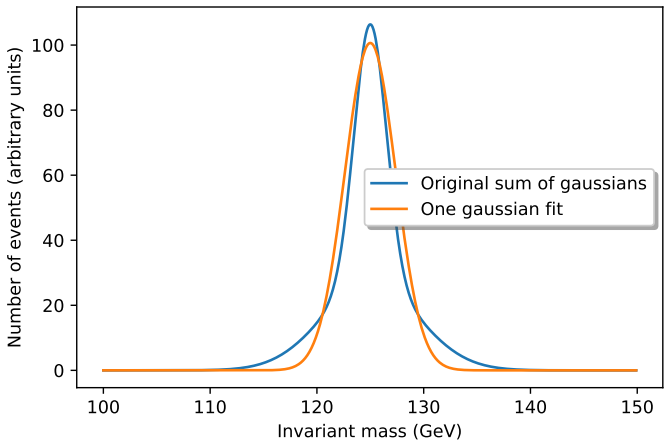


Figure 2.5: Sum of Gaussians where $\frac{\Delta m}{r} = 0$, $\frac{\sigma_1}{\sigma_2} = 1$, $\frac{\sqrt{r^2+\Gamma_2^2}}{\sqrt{r^2+\Gamma_1^2}} = 3$ and $\chi^2 = 11.1$.

We can also check to see if equation (2.11) still holds in the case where the decay width is non-negligible. To do this, we run a code to find the largest value for $|m_w - \mu|$ over the points where $\chi^2 < 1$ and we find that

$$|m_w - \mu|_{max} = 0.23r \tag{2.16}$$

where $r$ is the experimental resolution. Therefore, the approximation in equation (2.11) still holds for all the points fulfilling the single-particle assumption.

It would also be interesting to get an equivalent for equation (2.11), but for the decay widths instead of the masses. To do this, we define the weighted average of the variances of the two Gaussians as

$$s_w = \frac{\sigma_1 s_1 + \sigma_2 s_2}{\sigma_1 + \sigma_2}. \tag{2.17}$$

If we run a code to find the largest value for $|s_w - s|$ over the points where $\chi^2 < 1$, we find that

$$|s_w - s|_{max} = 0.38r. \tag{2.18}$$

This means that we can conclude that the approximation

$$s \approx \frac{\sigma_1 s_1 + \sigma_2 s_2}{\sigma_1 + \sigma_2} \tag{2.19}$$

is a fairly good approximation as long as the two Higgs bosons have properties that are consistent with the assumption of a single particle, even though this approximation is not quite as good as the one in equation (2.11).

## 2.3 Three Higgs Bosons

While we have up until now focused on cases where there are only two Higgs bosons, some models predict that there are three or more Higgs bosons. Therefore, it may be useful to look into the case where there are three Higgs bosons as well. We will not look into cases with more than three Higgs bosons, because that would become very complicated due to the large number of parameters. We will also reduce the number of parameters by using the narrow-width approximation.

If we add a third Gaussian signal to the two Gaussian signals we already had, equation (2.7) becomes

$$S(E) = L_{\text{int}} \left( \sigma_1 e^{-\frac{(E-m_1)^2}{2r^2}} + \sigma_2 e^{-\frac{(E-m_2)^2}{2r^2}} + \sigma_3 e^{-\frac{(E-m_3)^2}{2r^2}} \right). \tag{2.20}$$

Once again, we can include $\sigma_2$ in the overall normalization to reduce the three cross section to two parameters, $\frac{\sigma_1}{\sigma_2}$ and $\frac{\sigma_3}{\sigma_2}$. Similarly to before, we can also reduce the three masses and experimental resolution to two parameters, $\frac{m_2 - m_1}{r}$ and $\frac{m_3 - m_1}{r}$. As before, we assume without loss of generality that $m_2 \geq m_1$ and $m_3 \geq m_1$ (we do not assume anything about the ordering of $m_2$ and $m_3$). Therefore, we have four parameters: the two cross section ratios $\frac{\sigma_1}{\sigma_2}$ and $\frac{\sigma_3}{\sigma_2}$ and the two mass differences $\frac{m_2 - m_1}{r}$ and $\frac{m_3 - m_1}{r}$.

Since plotting in 4D space is very difficult, we can not plot the entire parameter space as we did before. Therefore, we will start by assuming that all three Higgs bosons have the same cross section, that is $\frac{\sigma_1}{\sigma_2} = \frac{\sigma_3}{\sigma_2} = 1$, and focus only on varying the mass differences. The result of doing this is shown in figure 2.6a.

We can see here that the fit is only good if all three Higgs bosons are close enough in mass. If at least one mass difference is larger than three times the experimental resolution, $\chi^2$ becomes very large. This can be compared to figure 2.1, where we see that if $\frac{\sigma_1}{\sigma_2} = 1$, then the fit is only good if the mass difference is less than the experimental resolution. So the fact that if two Higgs bosons have the same cross section, they must also have $\Delta m < r$ generalizes to three Higgs bosons as well.

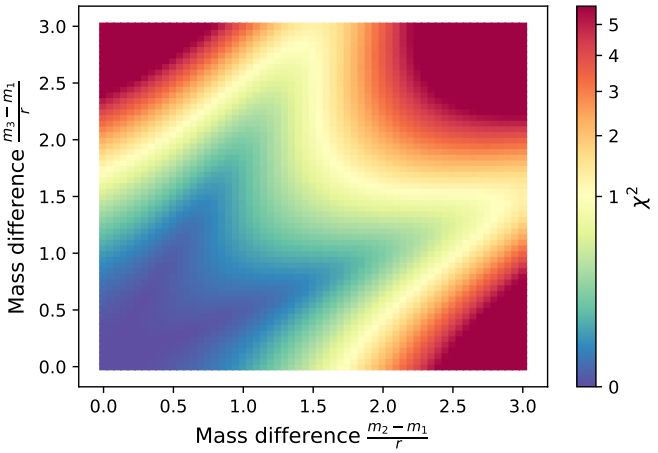


(a) All three Higgs bosons are assumed to have the same cross section.

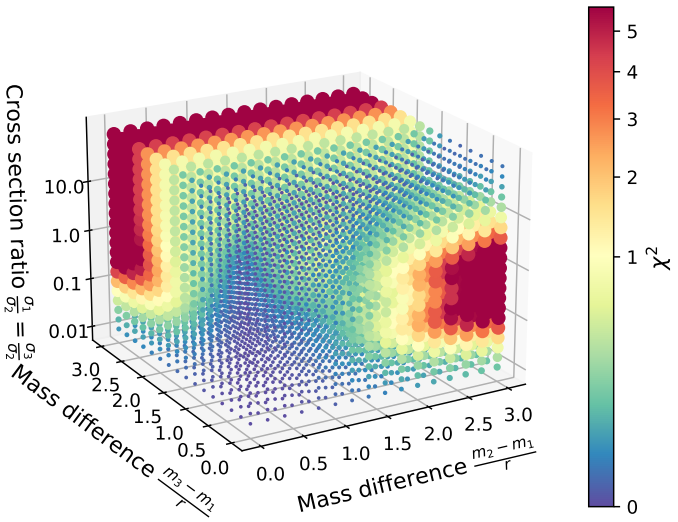


(b) Higgs bosons 1 and 3 are assumed to have the same cross section, the relative cross section of Higgs boson 2 varies along the $z$-axis.

Figure 2.6: $\chi^2$ of the Gaussian fit as a function of the mass differences between the three Higgs bosons.

We can also add a third dimension to figure 2.6a to see what happens when we assume that only two of the three Higgs bosons have the same cross section and let the cross section of the third Higgs bosons vary. This is shown in figure 2.6b.

If we look at the plane where $\frac{\sigma_1}{\sigma_2} = \frac{\sigma_3}{\sigma_2} = 1$, as expected, we can guess the same pattern as in figure 2.6a. By looking at the plane where $\frac{m_3 - m_1}{r} = 0$, we also see the same pattern as in figure 2.1. This is because if two of the three Higgs bosons have the same mass, their sum will be a perfect Gaussian, so it will look like we only have two Higgs bosons. However, the bump corresponding to Higgs bosons 1 and 3 will be twice as tall as the bump corresponding to Higgs boson 2, so that pattern is centered at $\frac{\sigma_1}{\sigma_2} = \frac{\sigma_3}{\sigma_2} = 0.5$ instead of 1 as in figure 2.1.

We also see that if $\frac{\sigma_1}{\sigma_2} = \frac{\sigma_3}{\sigma_2}$ is very small, then $\chi^2$ is very small no matter what. This is because that would mean that the bump corresponding to Higgs boson 2 is much larger than the two other bumps, so the two other bumps will be negligible compared to the bump for Higgs boson 2.

If $\frac{\sigma_1}{\sigma_2} = \frac{\sigma_3}{\sigma_2}$ is very large, then we see that $\chi^2$ is small if and only if $m_1 - m_3$ is small. This is because in that case the bump corresponding to Higgs boson 2 is much smaller than the two other, so it will look like there are only two Higgs bosons, 1 and 3, with the same amplitude. The only way $\chi^2$ can be small in that case if those two Higgs bosons are very close in mass.

Up until now, we have assumed that at least two of the three cross sections are equal. In order to get a complete picture of what happens when we vary the cross sections, we will now vary the two cross section ratios $\frac{\sigma_1}{\sigma_2}$ and $\frac{\sigma_3}{\sigma_2}$ and assume that three Higgs bosons are evenly separated in mass with a separation equal to twice the experimental resolution and $m_1 < m_2 < m_3$. The result of doing this is shown in figure 2.7a.

We can see that $\chi^2$ is the smallest in the three corners which correspond to one cross section being much larger than the two others, causing the bump for that Higgs boson to be much larger than the two other bumps. The red lines in the middle are where no single cross section is dominant over the two others. This generalizes the fact that for two Higgs bosons $\chi^2$ is always small if one of the Higgs bosons has a much larger cross section than the other.

We can also make a 3D plot out of this where we still assume that the masses are evenly spaced, but vary that spacing, as shown in figure 2.7b. As expected, we see that the closer the Higgs bosons get in mass, the smaller $\chi^2$ gets. We also see that if one of the Higgs bosons has a much larger cross section than the two others, $\chi^2$ will be small no matter how far apart the masses are.

As expected, we also see the same pattern as in figure 2.7a for large spacings, and the same pattern as in figure 2.1 if two of the Higgs bosons have a much larger cross section than the third.

So to conclude, what we have seen for two Higgs bosons generalizes to three Higgs bosons, that is that if the Higgs bosons have very different masses and similar cross sections $\chi^2$ will be large, and if one Higgs boson has a cross section that is dominant over the others $\chi^2$ will always be small.

As before, we can once again check if equation (2.11) still holds for three Higgs bosons. We find that the largest value for for $|m_w - \mu|$ over the points where $\chi^2 < 1$ is equal to

$$|m_w - \mu|_{max} = 0.21r. \tag{2.21}$$

We therefore conclude that the approximation in equation (2.11) still holds in cases where there are three Higgs bosons, though it is slightly worse than in the case where there are two Higgs bosons.

# 3 Simulations

In this section, we will use the software MadGraph [10] to simulate what the detector would actually see if there are multiple Higgs bosons, and compare the results to the simplified view

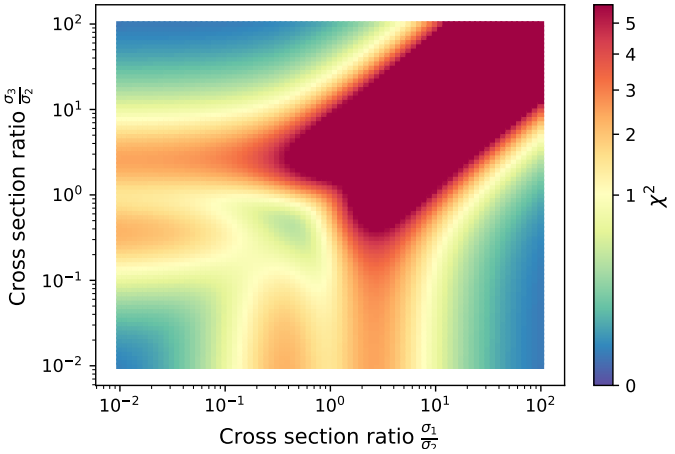


(a) The masses are assumed to be evenly spaced with a spacing equal to twice the experimental resolution.

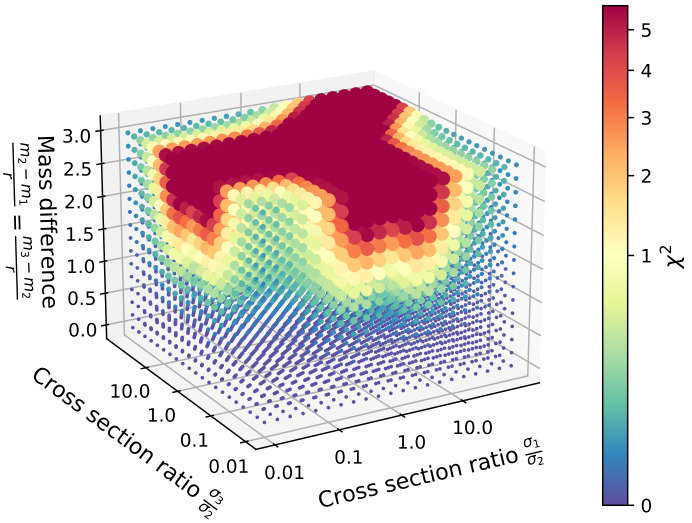


(b) The masses are assumed to be evenly spaced with spacing specified by the $z$-axis.

Figure 2.7: $\chi^2$ of the Gaussian fit as a function of the cross section ratios between the three Higgs bosons.

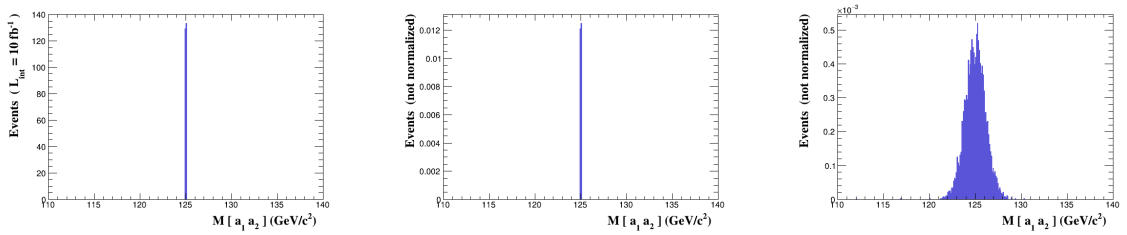


(a) Generator level (b) Hadron level (c) Reconstruction level

Figure 3.1: Invariant mass distribution of the photons in the Standard Model simulations of the process $pp \to h \to \gamma\gamma$.

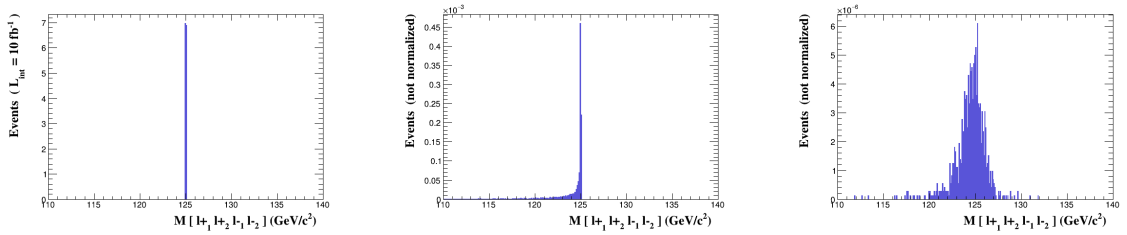


(a) Generator level (b) Hadron level (c) Reconstruction level

Figure 3.2: Invariant mass distribution of the leptons in Standard Model simulations of the process $pp \to h \to \ell^+\ell^+\ell^-\ell^-$, where $\ell$ can be electrons, muons or both.

discussed in the previous section.

## 3.1 Single-Particle Simulations

Since we want to see which combinations of multiple Higgs bosons look like a single Higgs boson to the detectors, we first need to know what the detectors see when there is a single Higgs boson in order to have something to compare to.

We start by running simulations of three selected LHC processes of single Higgs production. These processes are $pp \to h \to \gamma\gamma$ and $pp \to h \to \ell^+\ell^+\ell^-\ell^-$ because those have very clean experimental signatures, and $pp \to h \to b\bar{b}$ because that is one of the most common decay modes for most Higgs bosons. The results of the simulations for these processes are shown in figures 3.1-3.3. All three processes start with proton proton collisions at the 13 TeV LHC.

The simulations are run using MadGraph 5 version 2.9.3 [10], and the plots are generated using MadAnalyis 5 version 1.8.45 [11, 12, 13, 14, 15, 16]. We use the `heft` model to simulate the effective Higgs-gluon and Higgs-photon couplings resulting from top quark and W loops. MadGraph itself only does generator level simulations, but interfaces to Pythia 8.2 [17] for hadron level simulations. Pythia does not output jets but individual hadrons, so we use the MadAnalysis default reconstruction to see what the events would look like to a perfect detector, and that is what we call hadron level. Based on the hadron level events, we perform reconstruction level simulations using Delphes 3.4.2 [18]. For the reconstruction level simulations, we use the default Delphes configuration for the ATLAS detector.

We start by running simulations for a Standard Model Higgs boson with mass equal to 125 GeV. The results of these simulations are shown in figure 3.1 for $H \to \gamma\gamma$, in figure 3.2 for $H \to 4l$, and in figure 3.3 for $H \to b\bar{b}$.

We notice that for all three processes, the generator level distributions (figures 3.1a-3.2a) all show

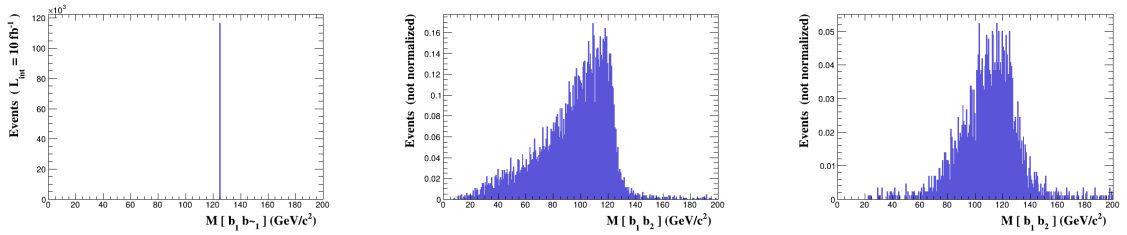


(a) Generator level (b) Hadron level (c) Reconstruction level

Figure 3.3: Invariant mass distribution of the bottom quarks or jets in Standard Model simulations of the process $pp \to h \to b\bar{b}$.

extremely narrow peaks around 125 GeV. This is expected since the only thing that could broaden the peaks in those cases is the decay width of the Higgs boson, which is predicted to be around 4 MeV, while the plots are on the GeV scale. Also, we see that all these three figures look almost identical (figure 3.3a only looks different at first sight because the $x$-axis has a different scale). This is expected since the decay products of the Higgs boson will always have an energy equal to the mass of the Higgs boson, no matter what types of particles these decay products are.

We see very few effects on the photons and leptons in the hadron level distributions (figures 3.1b and 3.2b). This is because photons and electrons do not decay, and muons have a lifetime much longer than the time it takes for them to reach the detector. The small effects that we see to the left of the peak in figure 3.2b which is not there in figure 3.2a is most likely due to bremsstrahlung, that is very energetic leptons emitting photons and slowing down.

In figure 3.3b, however, we see a large effect. This is because the bottom quarks and their decay products will hadronize and form jets. Often the jets will themselves emit more jets, and since figure 3.3b only shows the two most energetic b-jets this means that a lot of energy will not be detected. The reason we only want to plot the two most energetic jets is because in reality there will also be a lot of background jets due to proton collisions that have nothing to do with Higgs bosons, and plotting those as well would make it very difficult to see anything interesting.

We also see in the reconstruction level distributions (figures 3.1c-3.2c) that the peaks are broadened. This is due to the effect explained in the introduction that the detectors are not perfect and will often show energies slightly lower or slightly higher than the true energies. This is especially noticeable in figure 3.1c where what was a very clean and narrow peak without detector effects became a Gaussian. We also notice in figure 3.3c that in addition to there being events at higher invariant masses (which were very rare in figure 3.3b), there are also very few events at very low invariant masses, even though there were quite a few such events without detector effects. This is most likely due to it being more difficult to efficiently find which jets originated from bottom quarks if the jets have low energy.

We can also see in figure 3.1c that the per-bin uncertainty is typically around $5 - 10\%$ of the amplitude of the Gaussian. In equation (2.8), we assumed that the uncertainty is 1.3% of the total amplitude. While we do not know the actual uncertainty since we are simulating an arbitrary number of events, 1.3% is much less than $5 - 10\%$, so it is a reasonable lower estimate for the uncertainty. So we considered experimental analyses with significantly fewer fluctuations than the plots we are showing here. The reason we did not generate more events until we reached the 1.3% uncertainty is because it would take significantly more time without any qualitatively new insights.

## 3.2 Two Higgs Bosons with Large Mass Difference and Same Coupling

Now that we know how the plots look for the Standard Model, we can simulate the corresponding plots for models with multiple Higgs bosons. For this we will use the TRSM model [19], though in order to simulate cases with only two Higgs bosons, we will assume that the third Higgs boson does not interact with other particles at all. It would in principle be possible to use the third Higgs boson as well, but we will not do that because, as we will see, two Higgs bosons will already give a good picture of what happens in different cases, and adding a third Higgs boson will not really teach us anything new. We avoid interference by working in the narrow width approximation. Interference effects will be studied in the next section.

We will start with a case where it should be obvious that there are two Higgs bosons, that is a point in red in figure 2.1. We choose the point where $\frac{\Delta m}{r} = 5.3$ and $\frac{\sigma_1}{\sigma_2} \approx 1$.

Since the MadGraph input takes the masses of the Higgs bosons in GeV as opposed to units of the experimental resolution as given by figure 2.1, we first need to determine the experimental resolution. This can easily be done by looking at figure 3.1c, where we can see that the experimental resolution is about 1.5 GeV. Therefore, to get $\frac{\Delta m}{r} = 5.3$, we need $\Delta m = 8\,\text{GeV}$, so we choose $m_1 = 121\,\text{GeV}$ and $m_2 = 129\,\text{GeV}$.

We also want to fix $\frac{\sigma_1}{\sigma_2}$. The couplings of the Higgs boson $h_j$ (where $j$ is 1 or 2) in the TRSM model is scaled by a factor of $\kappa_j$ relative to the Standard Model. The MadGraph input does not take the cross sections but the coupling constants, so instead of setting $\sigma_1/\sigma_2 = 1$, we set $\kappa_1^2/\kappa_2^2 = 1$. The square comes from the fact that the matrix element must be squared when calculating the cross section, the reason why this is not a fourth power (where another square would come from the fact that there are two couplings) is because in the narrow width approximation, where the Higgs boson is exactly on-shell, we can factor:

$$\sigma_{\text{total}} \approx \sigma_{\text{prod}} \cdot BR \tag{3.1}$$

where $\sigma_{\text{prod}}$ is the production cross section and $BR$ is the branching ratio. There is one factor of $\kappa$ in $\sigma_{\text{prod}}$, but the branching ratio does not contain any $\kappa$. The cross section ratio and coupling ratio are very similar, but they are not necessarily equal as we will see, so by setting $\frac{\kappa_1^2}{\kappa_2^2} = 1$, we only get $\frac{\sigma_1}{\sigma_2} \approx 1$.

So we set $m_1 = 121\,\text{GeV}$, $m_2 = 129\,\text{GeV}$ and $\kappa_1^2 = \kappa_2^2$, and run the simulation. The results of this simulation are shown in figures 3.4-3.6. If we now look at figures 3.4c and 3.5c, we can clearly see two peaks, which means that there are clearly two Higgs bosons. This is consistent with the fact that we chose a point in red in figure 2.1.

First of all, we notice that even though we set the coupling constants of the two Higgs bosons to be equal, the peaks do not have equal heights, which means that the cross sections are not equal. The main reason for this in the $H \to 4l$ case is that even though the vertex terms in the Feynman diagrams are equal, the propagator terms are not. In the case where the Higgs bosons decay into four leptons, at least one of the intermediate Z-bosons needs to be off-shell for the chosen Higgs masses. Since more energy is available when the heavier Higgs boson decays than when the lighter Higgs boson decays, the heavier Higgs boson has slightly less trouble producing the off-shell Z-boson, which makes the process $h_2 \to \ell^+\ell^+\ell^-\ell^-$ more likely than $h_1 \to \ell^+\ell^+\ell^-\ell^-$, which is why the second peak in figure 3.5a is slightly higher than the first peak. The same behavior is observed in the Standard Model [20].

For the $H \to \gamma\gamma$ process, we see the opposite effect, that is that the peak for $h_1 \to \gamma\gamma$ is slightly taller than the one for $h_2 \to \gamma\gamma$. Just like in the Standard Model [20], this loop-induced decay is not very sensitive to mass. Instead, the effect that is the most noticeable in the $H \to \gamma\gamma$ case is that the production cross sections are different. This is because creating a lighter Higgs boson requires less energy than creating a heavier Higgs boson, so it is slightly easier to create lighter Higgs bosons. This is why there are more events involving $h_1$ than $h_2$ for the $H \to \gamma\gamma$ case.

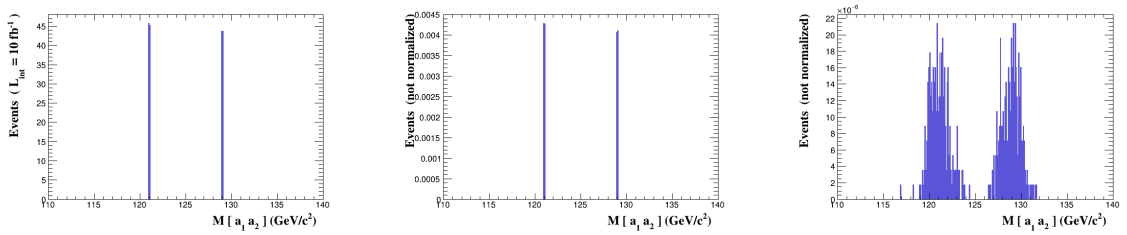


(a) Generator level (b) Hadron level (c) Reconstruction level

Figure 3.4: Invariant mass distribution of the photons in simulations of the processes $pp \to h_1 \to \gamma\gamma$ and $pp \to h_2 \to \gamma\gamma$ using $m_1 = 121\,\text{GeV}$, $m_2 = 129\,\text{GeV}$ and $\kappa_1^2 = \kappa_2^2$.

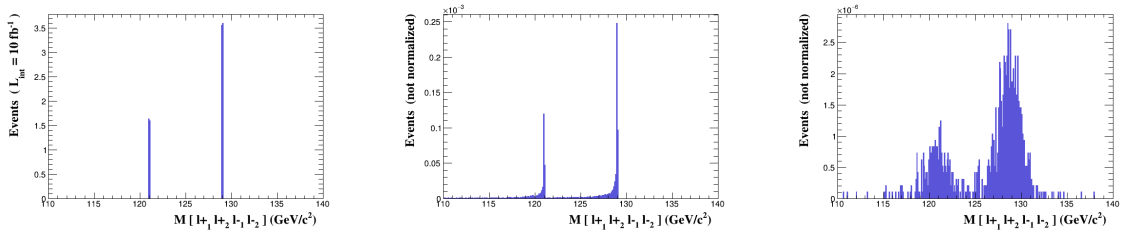


(a) Generator level (b) Hadron level (c) Reconstruction level

Figure 3.5: Invariant mass distribution of the leptons in simulations of the processes $pp \to h_1 \to \ell^+\ell^+\ell^-\ell^-$ and $pp \to h_2 \to \ell^+\ell^+\ell^-\ell^-$ using $m_1 = 121\,\text{GeV}$, $m_2 = 129\,\text{GeV}$ and $\kappa_1^2 = \kappa_2^2$. $l$ can be electrons, muons or both.

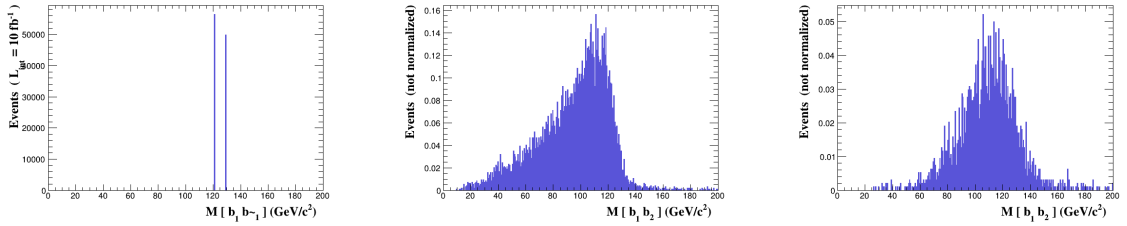


(a) Generator level (b) Hadron level (c) Reconstruction level

Figure 3.6: Invariant mass distribution of the bottom quarks or jets in simulations of the processes $pp \to h_1 \to b\bar{b}$ and $pp \to h_2 \to b\bar{b}$ using $m_1 = 121\,\text{GeV}$, $m_2 = 129\,\text{GeV}$ and $\kappa_1^2 = \kappa_2^2$.

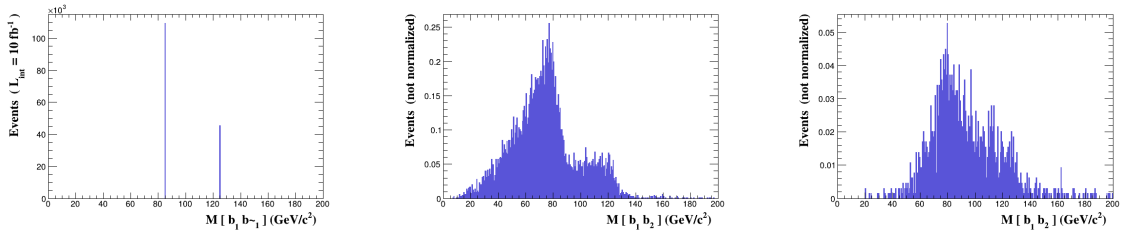


(a) Generator level (b) Hadron level (c) Reconstruction level

Figure 3.7: Invariant mass distribution of the bottom quarks or jets in simulations of the processes $pp \to h_1 \to b\bar{b}$ and $pp \to h_2 \to b\bar{b}$ using $m_1 = 85\,\text{GeV}$, $m_2 = 125\,\text{GeV}$ and $\kappa_1^2 = \kappa_2^2$.

Similarly, in figure 3.6a, the peak for $h_1 \to b\bar{b}$ is larger than the one for $h_2 \to b\bar{b}$, that is that the peak corresponding to the lighter Higgs boson is slightly taller than the peak corresponding to the heavier Higgs boson. The reason for this is because the branching ratio is equal to $\Gamma^j_{b\bar{b}}/\Gamma^j_{\text{total}}$, and while $\Gamma^j_{b\bar{b}}$ is not very sensitive to mass, $\Gamma^j_{\text{total}}$ increases quickly with mass due to decays into W- and Z-bosons.

Since $\kappa$ is the factor between the Standard Model coupling and the TRSM coupling, the only difference between the cross section of a Standard Model Higgs boson with mass $m$ (where $m$ does not have to be 125 GeV) and the cross section of a TRSM Higgs boson with the same mass $m$ is a factor of $\kappa^2$ (the square coming from squaring the matrix element), which means that

$$\begin{aligned} \sigma_j &= \kappa_j^2 \sigma_{\text{SM}} \\ \implies \frac{\sigma_1}{\sigma_2} &= \frac{\kappa_1^2}{\kappa_2^2} \frac{\sigma_{1\text{SM}}}{\sigma_{2\text{SM}}} \end{aligned} \tag{3.2}$$

which means that the ratio between the cross section ratio and the coupling ratio is simply the ratio of the cross sections for two Standard Model Higgs bosons with the given masses. Since the cross sections for Standard Model Higgs bosons are well known, even for Higgs bosons having masses different from 125 GeV, the factor $\frac{\sigma_{1\text{SM}}}{\sigma_{2\text{SM}}}$ is also well known. We could use the known $\sigma_{1\text{SM}}$ and $\sigma_{2\text{SM}}$ to find values for the $\kappa$'s for which $\sigma_1 = \sigma_2$ (rather than $\kappa_1^2 = \kappa_2^2$), but we will not do that since it does not change much.

If we look figure 3.6c, however, it is very difficult to see any difference whatsoever from the Standard Model behavior (figure 3.3c). Therefore, in the rest of this thesis, we will not bother simulating any more $H \to b\bar{b}$ decays, as they will all look very similar to the ones we have already plotted.

It could be interesting though to see what it looks like when the Higgs bosons are far enough apart to be resolved even by bottom quarks. This is shown in figure 3.7. In figure 3.7b, we can clearly see that there are two Higgs bosons since there are clearly two peaks, one on the right and one in the middle. In figure 3.7c, this is slightly less clear but is still not difficult to see. We also notice in figure 3.7a that even though the couplings are equal, the two peaks have very different height. This is the same effect as the one discussed earlier for figure 3.6a, but the effects are more pronounced since the mass difference between the two Higgs bosons is larger.

For this reason, analyses in the $b\bar{b}$ final state are not done as bump hunts, they typically involve advanced multivariate analysis. This is another important reason why we will not go into any more detail about this process.

## 3.3 Two Unresolved Higgs Bosons

Now that we have seen what it looks like if we simulate points in red in figure 2.1, we will simulate more cases with unresolved Higgs bosons, that is points in blue in figure 2.1. We will start by simulating the case where the two Higgs bosons have the same couplings but are very close together. For this, we use $m_1 = 124.5\,\text{GeV}$ and $m_2 = 125.5\,\text{GeV}$, which leads to $\Delta m = 1\,\text{GeV} = \frac{2r}{3}$, where $r \approx 1.5\,\text{GeV}$ is the experimental resolution in the $H \to \gamma\gamma$ and $H \to 4l$ channels. As before, we also set $\kappa_1^2 = \kappa_2^2$.

The results of this are shown in figure 3.8. At first sight, the plots in figure 3.8 look very much like those for the Standard Model (figures 3.1c and 3.2c). If we look very carefully we can see that the peak is slightly more round and that the events extend slightly further from the center (by less than 1 GeV), but that is not obvious at all. If plots like these are seen in an experiment, it is very difficult to tell that there are two Higgs bosons. Therefore, experiments could very well have seen something like this and interpreted as there being only one Higgs boson.

If we look at figure 2.1, we see that the other region in blue corresponds to Higgs bosons that

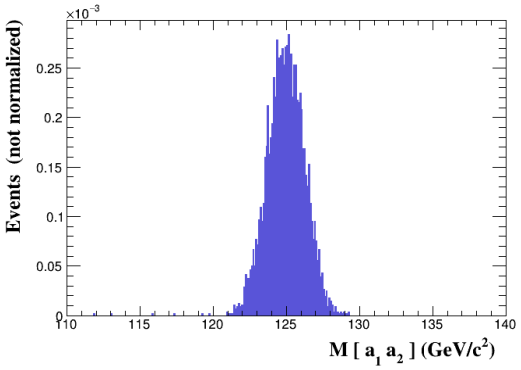


(a) $pp \to h_1 \to \gamma\gamma$ and $pp \to h_2 \to \gamma\gamma$.

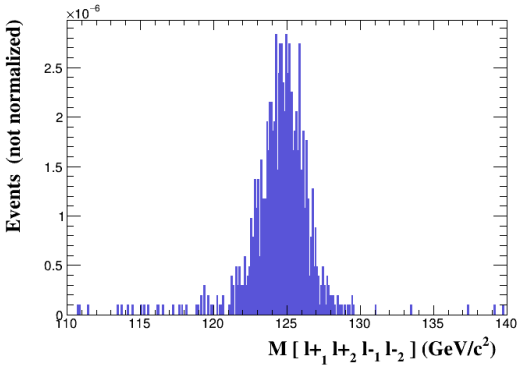


(b) $pp \to h_1 \to \ell^+\ell^+\ell^-\ell^-$ and $pp \to h_2 \to \ell^+\ell^+\ell^-\ell^-$.

Figure 3.8: Reconstruction level simulations of two studied signal processes, with $m_1 = 124.5\,\text{GeV}$, $m_2 = 125.5\,\text{GeV}$ and $\kappa_1^2 = \kappa_2^2$.

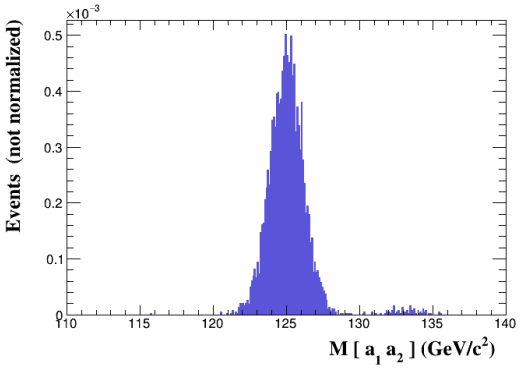


(a) Reconstruction level simulation of the processes $pp \to h_1 \to \gamma\gamma$ and $pp \to h_2 \to \gamma\gamma$.

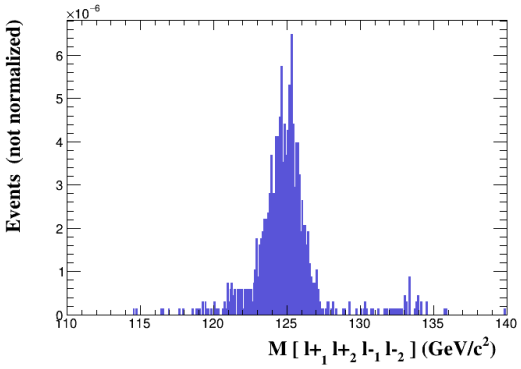


(b) Reconstruction level simulation of the processes $pp \to h_1 \to \ell^+\ell^+\ell^-\ell^-$ and $pp \to h_2 \to \ell^+\ell^+\ell^-\ell^-$.

Figure 3.9: Reconstruction level simulations of two Higgs bosons decaying into photons (figure 3.8a) or leptons (figure 3.8b), with $m_1 = 125\,\text{GeV}$, $m_2 = 133\,\text{GeV}$ and $\kappa_1^2 = 50\kappa_2^2$.

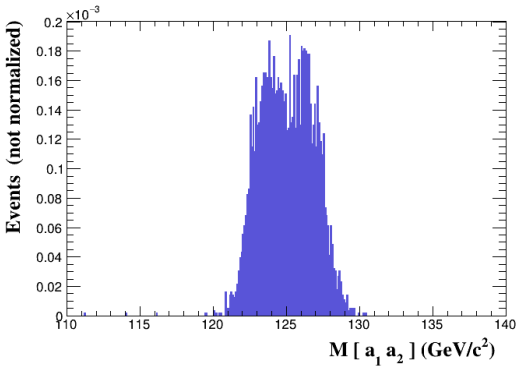


(a) Reconstruction level simulation of the processes $pp \to h_1 \to \gamma\gamma$ and $pp \to h_2 \to \gamma\gamma$.

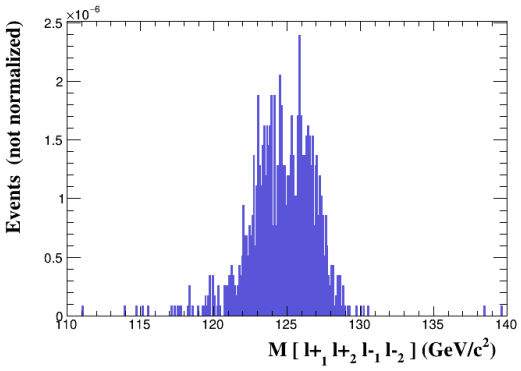


(b) Reconstruction level simulation of the processes $pp \to h_1 \to \ell^+\ell^+\ell^-\ell^-$ and $pp \to h_2 \to \ell^+\ell^+\ell^-\ell^-$.

Figure 3.10: Reconstruction level simulations of two Higgs bosons decaying into photons (figure 3.10a) or leptons (figure 3.10b), with $m_1 = 123.65\,\text{GeV}$, $m_2 = 126.35\,\text{GeV}$ and $\kappa_1^2 = \kappa_2^2$.

have very different mass but also very different cross sections. To simulate this case, we will set $m_1 = 125\,\text{GeV}$, $m_2 = 133\,\text{GeV}$, and $\kappa_1^2 = 50\kappa_2^2$, which corresponds to $h_1$ being the Standard Model Higgs boson and $h_2$ being a new Higgs boson which is more massive and interacts much less with matter. On figure 2.1, this corresponds to the point where $\frac{\Delta m}{r} = 4$ and $\frac{\sigma_1}{\sigma_2} \approx 50$.

The results of this are shown in figure 3.9. These plots look very much like those for the Standard model (figures 3.1c and 3.2c), except that there are some additional events between 130 GeV and 135 GeV. While this is clearly visible in figure 3.9, real experiments will have additional noise and background which is not present in the simulations, meaning that if experiments see cases like these they can easily interpret the second Higgs boson as noise or lose it in the background. Therefore, it is possible that there exists an additional Higgs boson of any mass (133 GeV was just an example, there is nothing special with that number) that has been missed because it couples very weakly to matter. This however has little to do with the main topic of this thesis, as detecting this additional Higgs boson does not involve resolving two Higgs bosons from one bump but rather searching for an entirely different particle with a lower cross section. It is only included here because it appears as an edge case in figure 2.1.

## 3.4 Borderline Cases

In figure 2.2, the Gaussians for borderline cases where $\chi^2 \approx 1$ are plotted. It would be interesting to see what those would actually look like to the detector, so we simulate cases where there are two Higgs bosons with those exact parameters. This means $m_1 = 123.65\,\text{GeV}$, $m_2 = 126.35\,\text{GeV}$ and $\kappa_1^2 = \kappa_2^2$ for figure 2.2a, and $m_1 = 125\,\text{GeV}$, $m_2 = 131\,\text{GeV}$ and $\kappa_1^2 = 20\kappa_2^2$ for figure 2.2b. The results of these simulations are shown in figures 3.10 and 3.11.

In figure 3.10, the two Higgs bosons are not clearly distinct, but the bump is clearly broader and more flattened on the top than the Standard Model one (figures 3.1c and 3.2c). This is similar to what we observe in figure 2.2a, where we can see that the sum of the two Gaussians (in blue) gives rise to a broader and more flattened bump than the single Gaussian (in orange).

In figure 3.11a, it is very clear that there are two Higgs bosons, just like it is very clear that the blue curve in figure 2.2b is not a single Gaussian (even without looking at the orange curve), while this is less clear in figure 3.11b. However, depending on how bad the background and noise are in the experiments, the second Higgs boson may or may not get lost in the background or be interpreted as noise. This is therefore again a case where our analysis will not tell us much, since detecting the new Higgs boson would involve detecting a new bump entirely rather than resolving

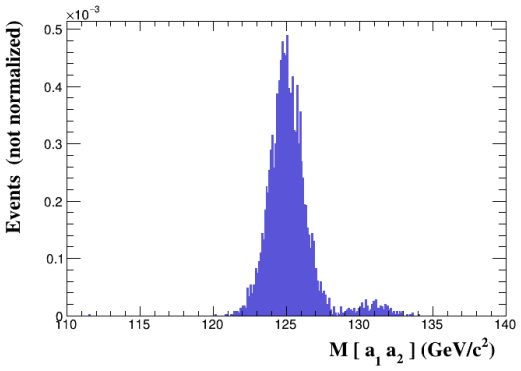


(a) Reconstruction level simulation of the processes $pp \to h_1 \to \gamma\gamma$ and $pp \to h_2 \to \gamma\gamma$.

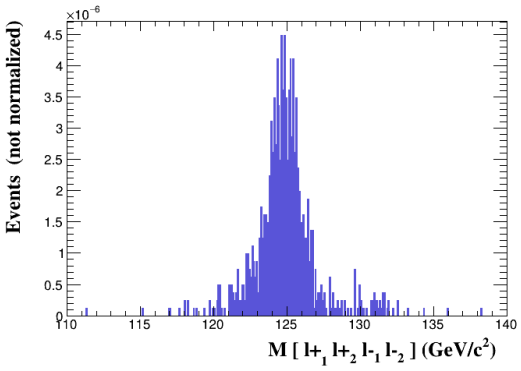


(b) Reconstruction level simulation of the processes $pp \to h_1 \to \ell^+\ell^+\ell^-\ell^-$ and $pp \to h_2 \to \ell^+\ell^+\ell^-\ell^-$.

Figure 3.11: Reconstruction level simulations of two Higgs bosons decaying into photons (figure 3.11a) or leptons (figure 3.11b), with $m_1 = 125\,\text{GeV}$, $m_2 = 131\,\text{GeV}$ and $\kappa_1^2 = 20\kappa_2^2$.

an additional Higgs boson in the already detected bump.

# 4 Interference and Non-Zero Width Effects

We have ignored interference so far, but in this section we will take a brief look at which effects interference could have on our analysis. We will start by explaining what interference is.

The cross section of a single process with a single Feynman diagram is proportional to the matrix element squared,

$$\sigma \propto |\mathcal{M}|^2 \tag{4.1}$$

where the matrix element $\mathcal{M}$ is the product of all the terms in the Feynman diagram.

In the simulations we have done up until now, for simplicity, we have treated the production and decay of both Higgs bosons as two separate processes, that is we generated the events for each process separately and then merged them together. This is equivalent to calculating the total cross section by summing up the individual cross sections:

$$\sigma_{\text{total}} = \sigma_1 + \sigma_2 \propto |\mathcal{M}_1|^2 + |\mathcal{M}_2|^2 \tag{4.2}$$

where $\sigma_1$ and $\sigma_2$ are the cross sections for $h_1$ and $h_2$ respectively. This means that we first squared the matrix elements and then summed them up.

However, in processes with the same initial and final states, equation (4.2) is not correct. The correct way to calculate the total cross section of such processes is to first add the matrix elements together, then square their sum:

$$\sigma_{\text{total}} \propto |\mathcal{M}_1 + \mathcal{M}_2|^2. \tag{4.3}$$

The fact that this is not simply equal to the sum of the individual cross sections is called interference. In our case, the processes $gg \to h_1 \to \gamma\gamma$ and $gg \to h_2 \to \gamma\gamma$ both have the same initial state (two gluons) and the same final state (two photons), and the same applies for the processes that produce leptons or bottom quarks. Therefore, to make a completely correct description of what is happening, we must take into account interference.

The absolute value squared of the sum of two complex numbers can be rewritten as

$$|\mathcal{M}_1 + \mathcal{M}_2|^2 = |\mathcal{M}_1|^2 + |\mathcal{M}_2|^2 + 2(\text{Re}(\mathcal{M}_1)\,\text{Re}(\mathcal{M}_2) + \text{Im}(\mathcal{M}_1)\,\text{Im}(\mathcal{M}_2)) \tag{4.4}$$

which means that the term

$$I = 2(\mathrm{Re}(\mathcal{M}_1)\,\mathrm{Re}(\mathcal{M}_2) + \mathrm{Im}(\mathcal{M}_1)\,\mathrm{Im}(\mathcal{M}_2)) \tag{4.5}$$

is the term that decides how large the interference is. This term can be either positive, in which case the interference is said to be constructive, or negative, in which case the interference is said to be destructive.

For the interference term to not be negligible, the decay width must be larger than the mass difference between the two particles. This is because for the interference term to be non-negligible, both matrix elements have to be non-negligible through some overlapping energy range.

## 4.1 Interference in the TRSM Model

In this thesis, we will look at the effects of interference on the $h \to \gamma\gamma$ process, as it is the simplest process to study. The $h \to ZZ \to 4l$ process has several particles with non-zero width making it more complicated, and as we saw in the previous section the $h \to b\bar{b}$ process does not produce any plots where it is easy to distinguish between the two Higgs bosons.

While Standard Model background processes can interfere with $gg \to h \to \gamma\gamma$ [21], since the background would be difficult to simulate, we will not treat signal background interference in this thesis.

In the TRSM model, the matrix element for the $gg \to H_j \to \gamma\gamma$ process is equal to

$$\mathcal{M}_j = C\frac{\kappa_j^2}{E^2 - m_j^2 + im_j\Gamma_j} \tag{4.6}$$

where one $\kappa_j$ comes from the coupling between the Higgs boson and the top loop connecting it to the gluons, the other $\kappa_j$ comes from the coupling between the Higgs boson and the top/W loop connecting it to the photons, $\frac{1}{E^2-m_j^2+im_j\Gamma_j}$ is the propagator term for the Higgs boson (where $E$ is the center of mass energy, which ends up being the invariant mass of the photons), and $C$ is a constant containing all the terms not related to Higgs bosons, such as the loop terms, the quark-gluon couplings and the quark-photon couplings. The reason we have a $\kappa^2$ here while we only had a $\kappa$ before is that now we are no longer using the narrow width approximation, so equation (3.1) is no longer valid, which means that the second $\kappa$ no longer cancels out.

By using the division rule for complex numbers, this matrix element can be rewritten in a way that allows us to easily see the real and imaginary parts:

$$\mathcal{M}_j = \frac{C\kappa_j^2}{(E^2 - m_j^2)^2 + m_j^2\Gamma_j^2}(E^2 - m_j^2 - im_j\Gamma_j). \tag{4.7}$$

By inserting this into equation (4.5), this gives us that the interference term between the two Higgs bosons is equal to

$$I = B\kappa_1^2\kappa_2^2((E^2 - m_1^2)(E^2 - m_2^2) + m_1m_2\Gamma_1\Gamma_2) \tag{4.8}$$

where

$$B = \frac{2C^2}{((E^2 - m_1^2)^2 + m_1^2\Gamma_1^2)((E^2 - m_2^2)^2 + m_2^2\Gamma_2^2)} \tag{4.9}$$

is always positive. Note that $B$ depends on $E$ and the properties of the Higgs bosons, so it is not constant. However, since it is always positive, it is still convenient to group all those terms into a single prefactor $B$.

This means that the interference is destructive if and only if $(E^2 - m_1^2)(E^2 - m_2^2) < -m_1m_2\Gamma_1\Gamma_2$. Since the masses and decay widths are always positive, $-m_1m_2\Gamma_1\Gamma_2$ is always negative, which

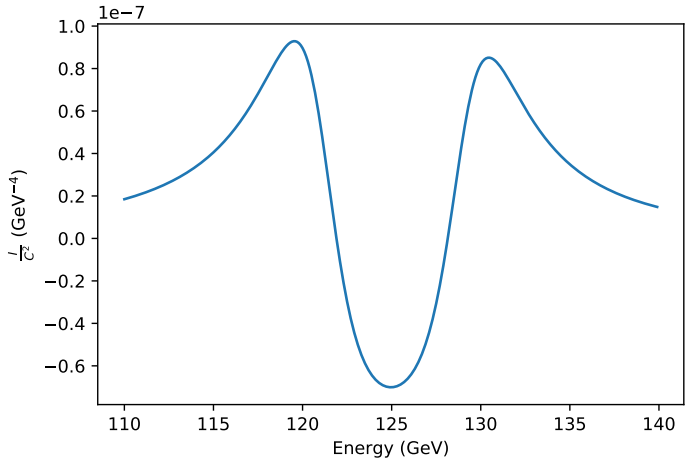


Figure 4.1: Interference term $\frac{I}{C^2}$ (where $C$ is the constant from equation (4.6)) as a function of the energy $E$ with $m_1 = 121\,\text{GeV}$, $m_2 = 129\,\text{GeV}$, $\Gamma_1 = \Gamma_2 = 5\,\text{GeV}$ and $\kappa_1 = \kappa_2$.

means that a necessary (but not sufficient) condition for the interference to be destructive is that $(E^2 - m_1^2)(E^2 - m_2^2)$ is negative, which can only happen if $E^2 - m_1^2$ and $E^2 - m_2^2$ have opposite signs. This means that in the TRSM model, the interference is always constructive outside of the two bumps, and can be destructive between the two bumps if the masses are far enough apart. The signs of the $\kappa$'s do not change anything, since they are real and the matrix element only depends on $\kappa^2$.

A plot of equation (4.8) using the same values for the masses and decay widths that we will use in the simulations is shown in figure 4.1.

However, in more complicated models, it is possible that each Higgs boson couples differently to different particles, so instead of having one overall $\kappa_j$ for Higgs boson $h_j$, we would have a $\kappa_{j,t}$ for its coupling to the top quark, a $\kappa_{j,W}$ for its coupling to the W-boson, etc. The only dominant loop that contributes to the effective coupling between Higgs bosons and gluons is a top loop, while both top and W loops contribute to the effective coupling between Higgs bosons and photons. This means that $\kappa_{j,g_{\text{eff}}}$ and $\kappa_{j,\gamma_{\text{eff}}}$ can be different, and in particular they can have different signs. This means that equation (4.8) becomes

$$I = B\kappa_{1,g_{\text{eff}}}\kappa_{1,\gamma_{\text{eff}}}\kappa_{2,g_{\text{eff}}}\kappa_{2,\gamma_{\text{eff}}}((E^2 - m_1^2)(E^2 - m_2^2) + m_1 m_2 \Gamma_1 \Gamma_2). \tag{4.10}$$

The main difference is that while in equation (4.8) the term $B\kappa_1^2\kappa_2^2$ was always positive, it is not possible to say anything general about the sign of the term $B\kappa_{1,g_{\text{eff}}}\kappa_{1,\gamma_{\text{eff}}}\kappa_{2,g_{\text{eff}}}\kappa_{2,\gamma_{\text{eff}}}$ in equation (4.10). This means that if this term is negative, it is possible to get the opposite effect as the one in the TRSM model, so the interference would be constructive between the two bumps and destructive outside.

While we would like to study such cases in this thesis, using these more complicated models in MadGraph is more difficult than using the TRSM model. However, to study such cases, it is not necessary to go into the details of a more complicated model, it is sufficient to make the pre-factor term negative. This can be done by editing the TRSM model to remove the $\kappa$ factor from the effective coupling between Higgs bosons and gluons, which means that equation (4.8) becomes

$$I = B\kappa_1\kappa_2((E^2 - m_1^2)(E^2 - m_2^2) + m_1 m_2 \Gamma_1 \Gamma_2). \tag{4.11}$$

While removing the $\kappa$ factors like this is very artificial, it allows us to mimic the behavior of more complicated models without having to go into the details of such models.

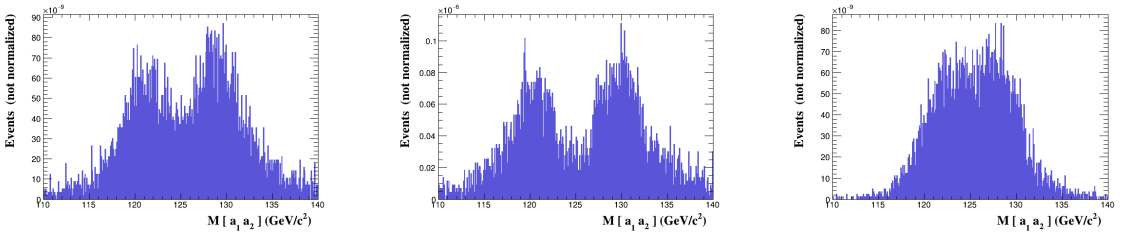


(a) No interference (b) Interference with $\kappa_1 = \kappa_2$ (c) Interference with $\kappa_1 = -\kappa_2$

Figure 4.2: Reconstruction level simulations of two Higgs bosons decaying into photons in the modified TRSM model, with $m_1 = 121\,\text{GeV}$, $m_2 = 129\,\text{GeV}$, $\Gamma_1 = \Gamma_2 = 5\,\text{GeV}$ and $\kappa_1^2 = \kappa_2^2$.

## 4.2 Invariant Mass Plots with Interference

In this subsection, we would like to see how interference can affect how easy it is to resolve two Higgs bosons.

In order for interference to be visible at all, the decay widths of the Higgs bosons must be large enough for their bumps to overlap even at the generator level. Otherwise, at any energy, at least one of the two matrix elements will always be negligible, which means that the interference term in equation (4.5) will always be very close to zero. Therefore, the decay width of the Standard Model Higgs boson, which is around 4 MeV, is too small as it would force us to put the two Higgs bosons much closer together than the experimental resolution, in which case we would not be able to distinguish them. For this reason, to be able see the effects of interference on the invariant mass plots, the Higgs bosons must have a decay width greater than the experimental resolution. Here, we will set their decay widths to be both equal to 5 GeV. This is of course just for illustration and such large widths for Higgs bosons around 125 GeV are excluded [22].

In order to be able to see what interference does to the invariant mass plots, we would like to look at a case where the two Higgs bosons are clearly distinct, that is a point in red in figure 2.1. As we saw in equation (2.15), if the two Higgs bosons have a non-negligible but equal decay width, figure 2.1 is still valid, but with an effective experimental resolution of $s = \sqrt{r^2 + \Gamma^2}$. In this case $r = 1.5\,\text{GeV}$ and $\Gamma = 5\,\text{GeV}$, which leads to an effective experimental resolution of $s = 5.2\,\text{GeV}$. If we set $\Delta m = 8\,\text{GeV}$ and $\kappa_1^2 = \kappa_2^2$, this means means that $\frac{\Delta m}{r} = 1.48$ and $\frac{\sigma_1}{\sigma_2} \approx 1$, which according to figure 2.1 should lead to two clearly distinct Higgs bosons.

Therefore, we run three simulations with $\Delta m = 8\,\text{GeV}$, $\Gamma_1 = \Gamma_2 = 5\,\text{GeV}$ and $\kappa_1^2 = \kappa_2^2$, one where we actively disable interference, one with interference with $\kappa_1 = \kappa_2$ and one with interference with $\kappa_1 = -\kappa_2$. The results of these simulations are shown in figure 4.2.

We see in figure 4.2b that setting $\kappa_1 = \kappa_2$ leads to the two Higgs bosons being more distinct. In figure 4.2b, the gap is much more pronounced than in figure 4.2a. This means that this type of interference makes the two Higgs bosons easier to distinguish.

For the case where $\kappa_1 = -\kappa_2$ (figure 4.2c), we see the opposite effect. While they were clearly distinct in figure 4.2a with a gap in the middle, they are much less distinct in figure 4.2c. Although the bump is still broad enough to not look like a single Gaussian, it is not as clear in figure 4.2c that there are two Higgs bosons as it is in figure 4.2a. Therefore, this type of interference makes the two Higgs bosons harder to distinguish.

This is to be expected since according to equation (4.11) and as shown in figure 4.1, the sign of the interference term can vary depending on whether the invariant mass is between the two Higgs masses or outside of the two Higgs masses. Here we clearly see that if $\kappa_1 = \kappa_2$, the interference is destructive in the center and constructive everywhere else, and the other way around for $\kappa_1 = -\kappa_2$.

One thing that is important to remember about the $\kappa$'s is that we are using a modified version of

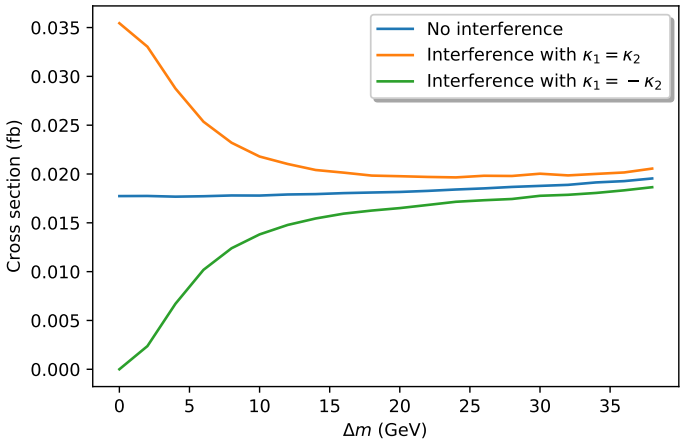


Figure 4.3: Total cross section of the processes $gg \to h_1 \to \gamma\gamma$ and $gg \to h_2 \to \gamma\gamma$ in the modified TRSM model as a function of the mass difference between the two Higgs bosons.

the TRSM model. In the TRSM model, the plots will always look like figure 4.2b regardless of the relative signs of the $\kappa$'s, and figure 4.2c can only be obtained in more complicated models.

## 4.3 Effects of Interference on Cross Sections

Now we know how interference affects the shape of the invariant mass plots, but it would also be interesting to know how interference affects the overall cross sections. To do this, we use MadGraph's scan feature to run simulations for different values of $\Delta m$ and plot the cross section as a function of $\Delta m$. The results of this are shown in figure 4.3.

We can see in figure 4.3 that in the case where $\kappa_1 = \kappa_2$, the overall interference is always constructive, whereas in the case where $\kappa_1 = -\kappa_2$ the overall interference is always destructive. This means that the interference on the outside has more effect on the overall cross section than the interference in the center.

We can also see that if $\Delta m = 0$, that is if the two Higgs bosons have exactly the same mass, the interference with $\kappa_1 = \kappa_2$ doubles the overall cross section, while the interference with $\kappa_1 = -\kappa_2$ reduces the overall cross section to a value very close to zero. This makes sense because if the two masses are equal, the propagator terms are equal (since we set the decay widths to be equal), and we set the couplings to be equal up to a sign difference, meaning that $\mathcal{M}_1 = \pm\mathcal{M}_2$. This means that according to equation (4.5), the interference term is equal to

$$I = \pm 2(\mathrm{Re}^2(\mathcal{M}) + \mathrm{Im}^2(\mathcal{M})) = \pm 2|\mathcal{M}|^2 \tag{4.12}$$

while the cross section without interference is equal to $|\mathcal{M}|^2 + |\mathcal{M}|^2 = 2|\mathcal{M}|^2$, which means that

$$I = \pm\sigma. \tag{4.13}$$

So if $I = \sigma$ the cross section gets doubled, while if $I = -\sigma$ the cross section gets reduced to zero.

If $\Delta m$ becomes very large, the cross sections with interference both approach the cross section without interference, which means that the interference term becomes very small. This makes sense because if the mass difference is much larger than the decay width, at least one of the two Higgs bosons will always become very off-shell, meaning that its matrix element will be very close to zero, meaning that the interference term will also be very small.

While the cross section without interference does not vary as much as the cross sections with interference, it does increase slightly with an increasing mass difference. This is simply due to the fact that we keep the mass average at 125 GeV, and if the mass difference is larger one Higgs boson must be lighter, and light Higgs bosons are easier to produce.

# 5 Conclusion

In this thesis, we have studied quasi-degenerate Higgs bosons and the circumstances under which they would appear as single particles to experimental searches and measurements.

In section 2, we first made the simplifying assumption that the distributions observed are exact Gaussians, and used a $\chi^2$ criterion to quantify how closely signals from multiple Higgs bosons resemble single-particle signals. We found that quasi-degenerate Higgs bosons with similar couplings with a mass separation less than twice the experimental resolution are very unlikely to be resolved by the experiments. If the couplings have different orders of magnitude though, the two Higgs bosons can be farther apart while still looking like one particle to the experiments. However, if they are too far apart, our analysis may not apply since then the question would be whether it is possible to detect particles with very weak couplings rather than whether the two bumps are actually separate. These results also generalize to cases with three Higgs bosons.

In cases with two Higgs bosons with non-negligible decay widths compared to the experimental resolution, these results only generalize if the two Higgs bosons have similar decay widths $\Gamma_1 \approx \Gamma_2 \approx \Gamma$. In this case, they can be treated as particles with narrow width with an experimental resolution equal to $\sqrt{\Gamma^2 + r^2}$, where $r$ is the actual experimental resolution. If the two Higgs bosons have significantly different decay widths, $\chi^2$ will be larger, which means that the two Higgs bosons are easier to distinguish.

We have also found that if the two Higgs bosons are close enough to be unresolved, then the bump will be centered at approximately the rate-weighted average of the masses of the two Higgs bosons like in equation (2.11). This also generalizes to cases where the two Higgs bosons have different decay widths and where there are three Higgs bosons. If the Higgs bosons have non-zero decay width, then similarly, if the two Higgs bosons are close enough to be unresolved, the weighted average of $\sqrt{\Gamma_1^2 + r^2}$ and $\sqrt{\Gamma_2^2 + r^2}$ will be approximately equal to the width of the bump.

In section 3, we compared our findings from section 2 to Monte Carlo simulations of some of the most important Higgs processes, $pp \to h \to \gamma\gamma$, $pp \to h \to ZZ \to 4l$ and $pp \to h \to b\bar{b}$. We first did Standard Model simulations to get a baseline, and then we used the TRSM model which is a simple singlet extension of the Standard Model Higgs sector to obtain invariant mass distributions of two quasi-degenerate Higgs bosons. We considered well-separated cases with $\chi^2 > 1$, unresolved cases with $\chi^2 < 1$, and borderline cases with $\chi^2 = 1$. We found that even though the shape of the bumps may be slightly different from what we assumed in section 2, the conclusions above still hold if the Higgs bosons have narrow decay widths.

If the two Higgs bosons have non-negligible decay widths, however, interference may need to be taken into account, which is what we did in section 4. In simple models like the TRSM model, interference will often be overall constructive and make the two Higgs bosons more distinct, but there can also be more complicated models with overall destructive interference making the two Higgs bosons less distinct. In order to be able to simulate overall destructive interference, we used a modified version of the TRSM model since the overall interference is always constructive in the TRSM model.

# References


[1] The ATLAS Collaboration, *Observation of a New Particle in the Search for the Standard Model Higgs Boson with the ATLAS Detector at the LHC* (2013)
https://arxiv.org/pdf/1207.7214.pdf

[2] The CMS Collaboration, *Observation of a new boson at a mass of 125 GeV with the CMS experiment at the LHC* (2013)
https://arxiv.org/pdf/1207.7235.pdf

[3] G. Arcadi, A. Djouadi and M. Raidal, *Dark Matter through the Higgs portal* (2019)
https://arxiv.org/pdf/1903.03616.pdf

[4] Stephen P. Martin, *A Supersymmetry Primer*, Department of Physics, Northern Illinois University, DeKalb IL 60115 (1998)
https://arxiv.org/pdf/hep-ph/9709356.pdf

[5] The CMS Collaboration, *Measurements of Higgs boson production cross sections and couplings in the diphoton decay channel at* $\sqrt{s} = 13\,\text{TeV}$ (2021)
https://arxiv.org/pdf/2103.06956.pdf

[6] The ATLAS Collaboration, *Search for resonances decaying into photon pairs in* $139\,\text{fb}^{-1}$ *of pp collisions at* $\sqrt{s} = 13\,\text{TeV}$ *with the ATLAS detector* (2021)
https://arxiv.org/pdf/2102.13405.pdf

[7] The CMS Collaboration, *Constraints on anomalous Higgs boson couplings to vector bosons and fermions in its production and decay using the four-lepton final state* (2021)
https://arxiv.org/pdf/2104.12152.pdf

[8] The ATLAS Collaboration, *Search for heavy resonances decaying into a pair of Z bosons in the* $\ell^+\ell^-\ell'^+\ell'^-$ *and* $\ell^+\ell^-\nu\bar{\nu}$ *final states using* $139\,\text{fb}^{-1}$ *of proton–proton collisions at* $\sqrt{s} = 13\,\text{TeV}$ *with the ATLAS detector*
https://arxiv.org/pdf/2009.14791.pdf

[9] P. Bechtle, S. Heinemeyer, T. Klingl, T. Stefaniak, G. Weiglein and J. Wittbrodt, *HiggsSignals-2: Probing new physics with precision Higgs measurements in the LHC 13 TeV era* (2020)
https://arxiv.org/pdf/2012.09197.pdf

[10] J. Alwall et al, *The automated computation of tree-level and next-to-leading order differential cross sections, and their matching to parton shower simulations* (2014)
https://arxiv.org/pdf/1405.0301.pdf

[11] E. Conte, B. Fuks and G. Serret, *MadAnalysis 5, a user-friendly framework for collider phenomenology*, Comput. Phys. Commun. 184 (2013)
https://arxiv.org/pdf/1206.1599.pdf

[12] E. Conte, B. Dumont, B. Fuks and C. Wymant, *Designing and recasting LHC analyses with MadAnalysis 5*, Eur. Phys. J. C 74 (2014)
https://arxiv.org/pdf/1405.3982.pdf

[13] B. Dumont, B. Fuks, S. Kraml et al, *Towards a public analysis database for LHC new physics searches using MadAnalysis 5*, Eur. Phys. J. C 75 (2015)
https://arxiv.org/pdf/1407.3278.pdf

[14] E. Conte and B. Fuks, *Confronting new physics theories to LHC data with MadAnalysis 5*, Int. J. Mod. Phys. A 33 (2018)
https://arxiv.org/pdf/1808.00480.pdf

[15] J. Y. Araz, M. Frank and B. Fuks, *Reinterpreting the results of the LHC with MadAnalysis 5: uncertainties and higher-luminosity estimates*, Eur. Phys. J. C 80 (2020)
https://arxiv.org/pdf/1910.11418.pdf

[16] J. Y. Araz, B. Fuks and G. Polykratis, *Simplified fast detector simulation in MadAnalysis 5* (2020)
https://arxiv.org/pdf/2006.09387.pdf

[17] T. Sjöstrand et al, *An Introduction to PYTHIA 8.2*, Comput. Phys.Commun. 191 (2015)
https://arxiv.org/pdf/1410.3012.pdf

[18] J. de Favereau et al, *DELPHES 3 - A modular framework for fast simulation of a generic collider experiment*, Centre for Cosmology, Particle Physics and Phenomenology, Université Catholique de Louvain, Belgium (2014)
https://arxiv.org/pdf/1307.6346.pdf

[19] T. Robens, T. Stefaniak and J. Wittbrodt, *Two-real-scalar-singlet extension of the SM: LHC phenomenology and benchmark scenarios* (2020)
https://arxiv.org/pdf/1908.08554.pdf

[20] D. de Florian et al, *Handbook of LHC Higgs cross sections: 4. Deciphering the nature of the Higgs sector*, LHC Higgs Cross Section Working Group (2017)
https://arxiv.org/pdf/1610.07922.pdf

[21] J. Song, Y. W. Yoon and S. Jung, *Interference effect on heavy Higgs resonance signal in $\gamma\gamma$ and $ZZ$ channels* (2016)
https://arxiv.org/pdf/1510.03450.pdf

[22] The CMS Collaboration, *Measurements of properties of the Higgs boson decaying into the four-lepton final state in pp collisions at* $\sqrt{s} = 13\,\text{TeV}$
https://arxiv.org/pdf/1706.09936.pdf